

PACS numbers: 02.30.Mv; 03.50.De; 07.05.Kf; 42.25.Gy; 42.82.Et
DOI: 10.1070/QE2010v040n09ABEH014332

Simulation of guided modes (eigenmodes) and synthesis of a thin-film generalised waveguide Luneburg lens in the zero-order vector approximation

A.A. Egorov, K.P. Lovetskii, A.L. Sevast'yanov, L.A. Sevast'yanov

Abstract. **Propagation of a guided mode (eigenmode) through an integrated optical generalised waveguide Luneburg lens is numerically simulated for the first time in terms of the previously obtained analytical solution of the vector electrodynamic problem in a smoothly irregular four-layer integrated optical 3D waveguide. The dispersion relation for a four-layer continuously irregular integrated optical 3D waveguide is calculated within the approximations of the asymptotic method of comparison waveguides and the method of adiabatic modes, in particular, taking into account the shift of the propagation constants of quasi-TE and quasi-TM modes. A generalised waveguide Luneburg lens with a full aperture is synthesised in the zero-order approximation. The results of numerical simulation demonstrate, on the one hand, a very good coincidence of the solution to the stated problem obtained in the approximation of the method of comparison waveguides with the previous results, and, on the other hand, advantages of our method: more rigorous solution of the problem, more complete consideration of its physical peculiarities, and higher accuracy of calculations. Another undoubted advantage of the analytical method proposed here is that it can be used to analyse similar structures fabricated of dielectrics, magnetics, and metamaterials, including nonlinear materials, in a wide range of electromagnetic wavelengths.**

Keywords: *irregular 3D waveguide, smooth irregularities, perturbation method, asymptotic method, generalised waveguide Luneburg lens, waveguide modes, dispersion relation.*

1. Introduction

In our previous studies [1 – 6] we obtained analytical expressions for the fields of distorted modes of a four-layer smoothly irregular integrated optical 3D waveguide in the zero- and first-order approximations of the perturbation theory using the asymptotic method and coupled-wave analysis. As the theoretical analysis showed, the smoothly irregular integrated optical waveguide has weakly hybrid quasi-TE and quasi-TM modes. The canonical (for the asymptotic method) form of the quasi-wave equations describing the structure of quasi-TE and quasi-TM modes in smoothly irregular four-layer integrated optical 3D waveguide was reported in [3, 4].

Our consideration was based on the solution in the form of a finite asymptotic series, known as the adiabatic approximation. The quasi-wave equations derived within the theoretical consideration were solved by the asymptotic method in the zero- and first-order approximations. In both cases we obtained an explicit dependence of the first-order small contributions to the amplitudes of electric and magnetic fields of quasi-waveguide modes and explicit expressions for the complex propagation constants of quasi-TE and quasi-TM modes. For real permittivity and permeability of the media in a smoothly irregular waveguide these shifts were found to be purely imaginary and different for different quasi-TE and quasi-TM modes [3].

There are at least two important problems in the integrated optics, which require to take into account the vector character of fields [1 – 13]. First, to implement effective energy transfer through different conjugation elements (lens, splitters, prisms, etc.), it is necessary to take into account the vector character of fields at all stages of solution of the electrodynamic problem of propagation of a plane monochromatic light wave in a multilayer integrated optical structure. The conjugation efficiency is known to depend strongly on the field matching before and after the conjugation element. Second, in some cases it is necessary to use an integrated optical device to perform an almost ideal Fourier transform, for example, in a real-time integrated optical high-frequency spectrum analyser operating on plane board [13]. This spectrum analyser must perform an instantaneous spectral analysis of the input radar signal to determine, for example, the object that tracks this plane (another plane, rocket, or ground-based radar). The signal spectrum at the analyser output is compared with the spectra stored in the board computer memory, due to which the pilot can timely take a correct decision.

Note that when passing to the nanoscale range, the requirements to the accuracy of calculating the parameters of similar waveguide devices become much more severe in view of the limitations imposed by diffraction effects

A.A. Egorov A.M. Prokhorov General Physics Institute, Russian Academy of Sciences, ul. Vavilova 38, 119991 Moscow, Russia; e-mail: yegorov@kapella.gpi.ru;
K.P. Lovetskii, A.L. Sevast'yanov, L.A. Sevast'yanov Peoples' Friendship University of Russia, ul. Miklukho-Maklaya 6, 117198 Moscow, Russia; e-mail: alsevastyanov@gmail.com, lovetskiy@gmail.com

Received 24 March 2010; revision received 10 July 2010
Kvantovaya Elektronika **40** (9) 830 – 836 (2010)
Translated by Yu.P. Sin'kov

[1–5, 9, 10, 13]. The latter determine to a great extent the accuracy of the Fourier transform performed by the lens and, correspondingly, the spectrum analyser resolution.

The classic Luneburg lens – a lens with a focal sphere coinciding with its surface [7–10] – was proposed by Luneburg in 1944. The dependence of the lens refractive index n on the distance r from the centre has the form $n(r) = \sqrt{2 - r^2}$. The focal distance of the lens is unity, and the n and r values are normalised to unity at the lens edge (r is normalised to the lens radius R). The Luneburg lens has a spherical or cylindrical shape; its distinction from conventional lenses is that its refractive index is not constant but depends on the distance to its centre or axis (spherical and cylindrical Luneburg lenses, respectively). Generally the law of change in the refractive index n is chosen so as to make parallel rays passing through a classical Luneburg lens to focus at one point on the lens surface and rays emitted by a point source on the lens surface to form a parallel beam far from the lens. Thus, the Luneburg lens performs a perfect Fourier transform, whose time scale is determined by the speed of light in the lens material.

Wide application of Luneburg lenses in optics and, all the more, in integrated optics is hindered, on the one hand, by serious difficulties in developing an adequate electrodynamic theory and the corresponding algorithms and programs for calculating such lenses and, on the other hand, by technological difficulties in fabricating lenses with a variable refractive index, which generally determine their high cost. To simplify calculations and production technology, such lenses are sometimes composed of discrete elements (for example, cubes with different refractive indices).

The generalised Luneburg lens is a lens whose focal surface does not coincide with its real surface and is located at a distance $r > R$ from the lens centre. In this study we consider a thin-film generalised waveguide Luneburg lens (TGWLL), which is used, for example, as a part of integrated optical high-frequency spectrum analyser. The waveguide modes and their characteristics are analysed within the adiabatic-mode model in the zero- and first-order approximations of the asymptotic method. To compare our results with those of other researchers, we used a rougher matrix model of comparison waveguides, which is derived from the zero-order approximation of adiabatic-mode model by replacing the tangential boundary conditions on nonhorizontal portions of interfaces between the layers of integrated optical waveguide with approximate conditions, taking into account only the horizontal contributions of the exact boundary conditions and neglecting the vertical ones. We showed previously [4–6] that this model coincides with the model of comparison waveguides [11, 12].

2. TGWLL eigenmodes

The fields of adiabatic modes of a smoothly irregular waveguide, which are solutions to the Maxwell equations, have the form

$$\tilde{\boldsymbol{E}}(x, y, z, t) = \exp(\mathrm{i}\omega t)\frac{\boldsymbol{E}(x; y, z)}{\sqrt{\beta(y, z)}}\exp[-\mathrm{i}k_0\varphi(y, z)],$$

$$\tilde{\boldsymbol{H}}(x, y, z, t) = \exp(\mathrm{i}\omega t)\frac{\boldsymbol{H}(x; y, z)}{\sqrt{\beta(y, z)}}\exp[-\mathrm{i}k_0\varphi(y, z)], \quad (1)$$

where $\boldsymbol{E}$ and $\boldsymbol{H}$ are, respectively, the vectors of electric and magnetic fields (the tilde sign indicates their complex character); $\omega\sqrt{\mu\varepsilon} = nk_0$; n is the refractive index of the medium (layer); $\varepsilon = \varepsilon_r\varepsilon_0$ is the permittivity of the medium; $\mu = \mu_r\mu_0$ is the magnetic permeability of the medium; ε_r and μ_r are, respectively, the relative permittivity and permeability; ε_0 and μ_0 are, respectively, the dielectric and magnetic constants; $k_0 = 2\pi/\lambda = \omega/c$ is the modulus of the wave vector $\boldsymbol{k}_0$; λ is the monochromatic light wavelength in vacuum; c is the speed of light in vacuum; and $\beta(y, z) = [\beta_y^2(y, z) + \beta_z^2(y, z)]^{1/2}$ is the length (norm) of the 2D vector field $\boldsymbol{\beta}(y, z) = (\beta_y(y, z), \beta_z(y, z))^{\mathrm{T}}$, composed of the partial derivatives of the eikonal $\beta_y(y, z) = \partial\varphi/\partial y$, $\beta_z(y, z) = \partial\varphi/\partial z$.

The eikonal (phase) $\varphi(y, z) = \int^{y,z}\beta(y', z')\mathrm{d}s(y', z')$ in (1) is found using integration along rays after solving the dispersion relation and isolate calculation of the rays and wavefronts in the horizontal plane [1, 5]; $\mathrm{d}s = (\mathrm{d}y^2 + \mathrm{d}z^2)^{1/2}$ is the ray length element.

The object of our study is the integrated optical device based on a three-layer regular planar waveguide (Fig. 1). One or several additional waveguide layers with refractive indices higher or lower than that of the main waveguide layer are deposited on one or several individual portions of this waveguide. First we consider the case where 'ideal' TE or TM modes propagate at regular portions of integrated optical structure. When passing through an irregular portion, these modes undergo deformations of different kind: scale transformation of the standing wave structure in the vertical direction, caused by a change in the waveguide geometric parameters in the vertical direction; mode hybridisation, caused by the 3D nature of irregular portions and, correspondingly, the vector character of fields; partial mode injection into the substrate and coating layer, which is caused by irregularities; etc.

By the example of TGWLL we will restrict ourselves to consideration of small geometric irregularities of the additional waveguide layer ($|\partial h/\partial y| \ll 1$, $|\partial h/\partial z| \ll 1$) (see Fig. 1) and eigenmode deformations of the first two types and estimate the power loss for leaky modes (see below).

TE and TM eigenmodes can propagate through a regular waveguide portion along the z axis. The $x = h(y, z) = \mathrm{const}$ interface between the waveguide layer and air at the regular portion is horizontal, and the tangential plane at any point $(h(y, z), y, z)^{\mathrm{T}}$ coincides with the yz plane. The tangential boundary conditions are satisfied separately for the TE and TM modes:

$$H_z|_{h-0} = H_z|_{h+0},\ E_y|_{h-0} = E_y|_{h+0}, \quad (2)$$

and

$$E_z|_{h-0} = E_z|_{h+0},\ H_y|_{h-0} = H_y|_{h+0}. \quad (3)$$

respectively. At the interface $x = h(y, z)$ of an irregular waveguide portion at a point $(h(y, z), y, z)^{\mathrm{T}}$ the tangential plane is set by the equation $\mathrm{d}x - (\partial h/\partial y)\mathrm{d}y - (\partial h/\partial z)\mathrm{d}z = 0$ and generally does not coincide with the horizontal plane yz, set by the equation $1\mathrm{d}x - 0\mathrm{d}y - 0\mathrm{d}z = 0$. In this case, the tangential boundary conditions

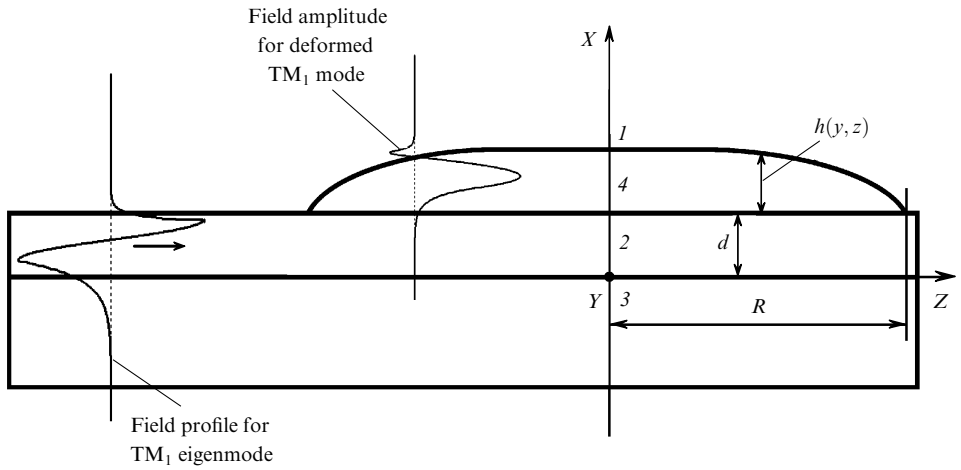

Figure 1. Cross section of the integrated optical structure under consideration: (*1*) environmental medium or coating layer (air) with refractive index n_c; (*2*) the first waveguide layer (regular part of the integrated optical structure) with refractive index n_f; (*3*) substrate with refractive index n_s; and (*4*) thin-film waveguide Luneburg lens (irregular part of the integrated optical 3D structure) with refractive index n_L (the second waveguide layer); $h(y, z)$ is the thickness of the Luneburg lens layer, R is the lens radius, and d is the thickness of the regular part of the waveguide integrated optical structure; the propagation direction of the TM_1 mode is shown by an arrow (on the left).

$$\boldsymbol{E}_\tau|_{h-0} = \boldsymbol{E}_\tau|_{h+0}, \quad \boldsymbol{H}_\tau|_{h-0} = \boldsymbol{H}_\tau|_{h+0} \tag{4}$$

are generally not satisfied separately for the TM and TE modes. Thus, specifically the boundary conditions relate two independent waveguide modes (the so-called quasi-TE and quasi-TM modes) into one weakly coupled hybrid mode. This coupling is weak in view of the estimate $|\partial h/\partial y|, |\partial h/\partial z| \ll 1$. The modes of a smoothly irregular waveguide, as well as the modes of a regular one, exhibit fast oscillations along the x axis; the number of these oscillations is retained during mode propagation.

3. Hierarchy of the matrix models of eigenmodes of an integrated optical multilayer smoothly irregular dielectric waveguide

In the zero-order approximation of the asymptotic method the quasi-wave equations for adiabatic modes [1] in each homogeneous layer take the form

$$\frac{\mathrm{d}^2 E_z^{(0)}}{\mathrm{d}x^2} + k_0^2(\varepsilon_j\mu_j - \beta^2)E_z^{(0)} = 0,$$
$$\frac{\mathrm{d}^2 H_z^{(0)}}{\mathrm{d}x^2} + k_0^2(\varepsilon_j\mu_j - \beta^2)H_z^{(0)} = 0. \tag{5}$$

The solutions to Eqns (5), with allowance for the boundary conditions at infinity ($|\boldsymbol{E}_{\tau(0)}|_{x\to\pm\infty} < +\infty$, $|\boldsymbol{H}_{\tau(0)}|_{x\to\pm\infty} < +\infty$), for the zero-order approximations of the waveguide mode components can be explicitly expressed in terms of the uncertain coefficients $\{A_j, B_j\}$ [3]. The tangential boundary conditions form a homogeneous system of linear algebraic equations for the amplitude coefficients $\{A_j, B_j\}$ [1–5], which has a nontrivial solution if the determinant of the system matrix is zero.

Both the matrix $\hat{M}(\beta)$ and its determinant $\det(\hat{M}(\beta))$ depend on the real parameter $\beta \in [n_s, n_L]$. The dispersion equation $\det(\hat{M}(\beta)) = 0$ has the form of a nonlinear differential equation in partial derivatives with respect to h and an algebraic equation with respect to the vector field $\boldsymbol{\beta}$: $F_{\mathrm{disp}}(\beta, \beta_y, \beta_z; h, \partial h/\partial y, \partial h/\partial z; n_s, n_f, n_L, n_c; d) = 0$.

The adiabatic-mode model in the zero-order asymptotic approximation was used to study the TGWLL [7–10] by different authors with different success. Southwell's results [9, 10] appear to be most adequate.

Despite the significant progress in the computational technique and such numerical methods (used to solve many electrodynamic problems) as the finite-difference time domain (FDTD) method and its various modifications, up to now neither the problem of numerical simulation of hybrid-mode transmission through a TGWLL nor the problem of synthesising this lens even in the zero-order vector approximation could be solved. For example, Vekshin et al. [14], as well as some other researchers, instead of valuable analysis of the corresponding vector electrodynamic problem with allowance for the leaky-mode generation at the edges of the Luneburg lens, used the modified FDTD method to solve this problem within the formalism of TE and TM modes; i.e., did not take into account the vector character of hybrid modes in the lens.

The solution of the Maxwell equations by the FDTD method makes it possible to calculate efficiently the electromagnetic field in a limited region of space, for example, in a prism, cavity, diffraction grating, etc. Although this method is rather efficient and universal, it requires significant computational resources to solve the above-mentioned standard problems. When the problem is to calculate electromagnetic fields far from the object under study (for example, lens), which emits or scatters the electromagnetic field, even the modified FDTD method requires a very large amount of computations, as a result of which its efficiency drastically decreases (see, for example, [15]). The FDTD method also gives rise to such problems as the 'numerical dispersion' (which leads to errors in determining the phase velocity) and 'numerical anisotropy', at which waves propagating in different directions in an isotropic region have different wavenumbers in the grid model [15]. Note that there are no unified effective ways for calculating fields in the far zone based on the FDTD calculation of the near-zone field. This also holds true for leaky waves. Only a

limited class of problems that are of interest for the case under study [1–6, 9, 10, 13–18] can be effectively solved by the FDTD method.

In contrast to this technique, our method of adiabatic modes for calculating the dispersion relations and field distributions in smoothly irregular integrated optical 3D waveguides requires the operating memory and amount of computations several orders of magnitude smaller to obtain the same accuracy. At the same time, our method is free of such drawbacks as numerical dispersion and numerical anisotropy. To compare it with Southwell's approach, we used the matrix model of the method of comparison waveguides. It can be constructed by replacing the tangential conditions with their horizontal approximations, in which all terms containing the expressions $(\partial h/\partial y)$ and $(\partial h/\partial z)$ become zero, and the dispersion relation $\det(\hat{M}(\beta)) = 0$ becomes a transcendental algebraic equation with respect to h and $\beta = \beta_z$.

We established the advantage of the matrix model of our method over its conventional formulation. Specifically, we obtained the dispersion relations for three- and four-layer waveguides, which coincide with the dependences reported by Adams, Tamir, Kogel'nik, and other researchers for waveguides with coinciding parameters. The matrix model allowed us to obtain the dispersion relation in the form of a smooth continuous curve at a transition from three- to four-layer waveguide (Figs 2a, 2b), which could not be obtained within the conventional method of comparison waveguides.

An additional advantage of the matrix method of comparison waveguides is that it allows one to calculate the vertical distribution of the waveguide mode, which numerically demonstrates the conservation of the structure of a standing wave under its scale deformation. Note that waveguide modes are not hybridised within this model. This is quite natural, because the method of comparison waveguides uses not rigorous tangential boundary conditions but their horizontal projections, i.e., approximate boundary conditions, which make it possible to separately describe TE and TM modes.

4. Dispersion relation for TGWLL. Vertical distribution of the electromagnetic field of eigenmodes

The algorithm for calculating the dispersion relation in the matrix model of comparison waveguides was described in [4, 5]. Substituting the known solutions for the fields in each waveguide layer into the boundary conditions (disregarding the tilt of the additional layer surface), we obtain a homogeneous system of linear algebraic equations with respect to the amplitude coefficients, which determine the fields in the waveguide layers. The solvability condition for this system is the equality of its determinant to zero. In this case, the dispersion relation $\det(\hat{M}(\beta)) = 0$ is a transcendental algebraic equation at any values of horizontal coordinates (y, z), which coincides with the dispersion relation for a regular comparison waveguide at any (y, z) values. Using the calculated distributions of the phase lag coefficient $\beta(r)$, we calculate the corresponding $h(r)$ values of the thickness profile for the additional waveguiding TGWLL layer for all normalised radii $r \in [0, 1]$.

The algorithm for calculating the dispersion relation in the zero-order approximation of the adiabatic-mode model was described in [4, 5]. The expressions for the longitudinal field components E_z and H_z of the corresponding modes in the zero-oder (with respect to δ) approximation are used to calculate the solutions for E_y, H_x and E_x, H_y in the same approximation [1, 2, 5]. All these solutions contain the amplitude coefficients $\{A_j\}$ and $\{B_j\}$. In this approximation the dispersion relation is an algebraic polynomial equation with respect to the distribution of the lag coefficient $\beta^{(0)}(y, z)$, which is also considered in the zero-order approximation; therefore, $\beta(y, z) = \beta^{(0)}(y, z) + O(\delta)$.

Thus, all the components of the vertical distribution of quasi-waveguide modes $\boldsymbol{E}(x, y, z)$ and $\boldsymbol{H}(x, y, z)$ are calculated in the zero-order (with respect to δ) approximation at any values of the horizontal coordinates (y, z) with a specified distribution (profile) of the thickness $h(y, z)$ and for all vertical coordinates x. The algorithm for calculating the vertical field distribution in the matrix model of comparison waveguides and in the zero-order approximation of the adiabatic-mode model was described in [4, 5]. The consideration of the shift of the propagation constant [3] allows one to approximately calculate the component of the vertical distribution of quasi-waveguide modes $\boldsymbol{E}(x, y, z)$ and $\boldsymbol{H}(x, y, z)$ in the first-order (with respect to δ) approximation.

5. Results of numerical simulation

5.1 Calculation of the dispersion relations for a smoothly irregular four-layer integrated optical waveguide

Figure 2 shows the dependences of the effective refractive index (phase lag coefficient) β for the TM_0 mode on the thickness of waveguide layers for a four-layer integrated optical structure, calculated according to the matrix model of the method of comparison waveguides. This structure consists of a three-layer regular planar waveguide and a four-layer smoothly irregular waveguide (see Fig. 1), with the following parameters: substrate (SiO_2) refractive index $n_s = 1.470$; refractive index of the first (regular) waveguide layer (Corning 7059 glass) $n_f = 1.565$; refractive index of the second waveguide layer (Ta_2O_5 TGWLL) of variable thickness $h(y, z)$ $n_L = 2.100$; and refractive index of the coating layer (air) $n_c = 1.000$.

In the dispersion relations $\beta = \beta(d/\lambda, h/\lambda)$ the waveguide layer thicknesses are given in relative units (d/λ and h/λ), where $\lambda = 0.9$ μm. Thus, the left part of Fig. 2a (the interval on the abscissa axis approximately from 0 to 3) shows the dispersion relation for the three-layer regular waveguide, while the right part (the interval on the abscissa from 3.0 to 3.8) yields the dispersion relation for the four-layer smoothly irregular waveguide, containing a TGWLL.

The dependence $\beta(h/\lambda)$ is shown in Fig. 2b. The portions in the dispersion relation after $d/\lambda \simeq 3.0$ and at $h/\lambda \simeq 0 - 0.24$ correspond to some transient regime in a TGWLL. We obtained similar dispersion relations for modes of other types.

Figure 2c shows the same dependence as in Fig. 2a but for the TE_3 mode. Our preliminary analysis showed that the presence of steps in the dispersion relations, similar to those in Fig. 2c, can be explained by the partial power redistribution in the layers of the multilayer waveguide structure with a smoothly varied thickness of the additional waveguide layer (i.e., the lens). To determine the propagation constant and, correspondingly, β, one must solve the dispersion (or characteristic) equation, which explicitly

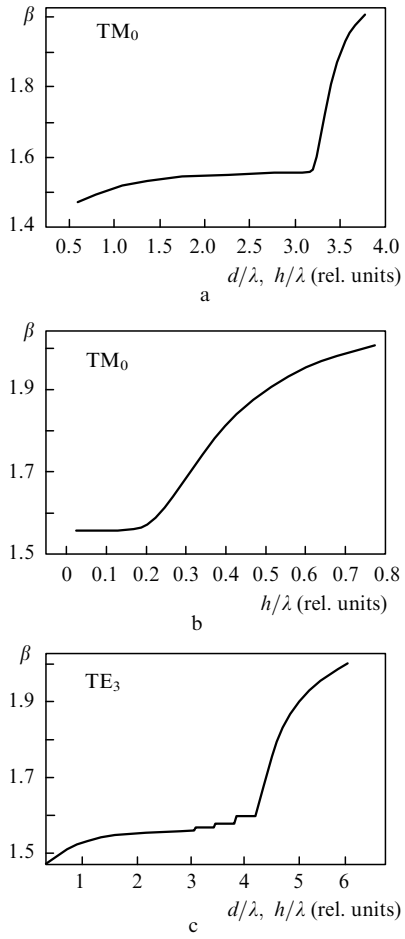

Figure 2. Dispersion relations of the integrated optical four-layer structure (Fig. 1) for the (a) TM_0 mode and (c) TM_3 mode and the dependence of β on the thickness of the second waveguide layer.

relates β and power distribution in a multilayer nonabsorbing waveguide in the integral form [16]:

$$\beta \approx \frac{\int_{S_\infty} n^2[\boldsymbol{E}_j \times \boldsymbol{H}_j^*]\boldsymbol{z}\,\mathrm{d}S}{\int_{S_\infty} n^2|\boldsymbol{E}_j|^2\,\mathrm{d}S}, \qquad (6)$$

where S_∞ is the area of infinite cross section; $\boldsymbol{E}_j$ amd $\boldsymbol{H}_j$ are the amplitudes of the electric and magnetic fields of the mode; and $\boldsymbol{z}$ is the unit vector of the z axis; $|\boldsymbol{E}_j|^2 = \boldsymbol{E}_j\boldsymbol{E}_j^*$. The integral in the numerator contains the total mode power, and the integral in the denominator contains in essence the total time-averaged energy per unit length of the waveguide structure for the jth mode, which propagates in the forward direction.

As follows from (6), a redistribution in the energy fluxes within one mode, propagating along the z axis, should affect the β value, which is observed in Fig. 2c. Indeed, a change in the parameters of the thin-film layer where the field (and, therefore, the power transferred through the waveguide) is mainly concentrated, should decisively affect the dispersion relation and the form of the fields in the corresponding regions of dispersion relations. A more detailed analysis of these phenomena is beyond the scope of this study.

Note that plots similar to that in Fig. 2c were reported in some publications but without explaining the mathematical and physical nature of the step dispersion relations for modes of order higher than TE_0 or TM_0 (see, for example, [18]).

5.2 Synthesis of a thin-film generalised waveguide Luneburg lens

Figure 3 shows the result of TGWLL synthesis (within the matrix method of comparison waveguides): the profile distribution $h(r)$ (r is the normalised lens radius, ranging from 0 to 1) was found for the normalised focal length $s = F/R$ (R is the radius of the TGWLL with a specified focal length F). This lens is described by the radial distribution $\beta(r, F)$ at $r \in [0, 1]$ in dimensionless radii R.

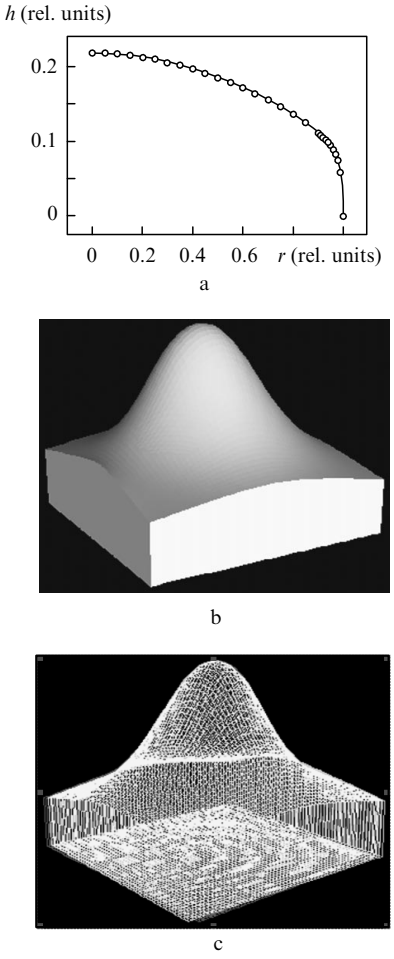

Figure 3. (a) Thickness profiles of generalised integrated optical Luneburg lenses with the focal length $s = 5$ (solid line indicates the results of our calculation and circles are Southwell's data), (b) 3D synthesised profile, and (c) a 3D stereogrid of the synthesised TGWLL thickness profile.

To compare our results with Southwell's data, we performed a calculation for a TGWLL with the following parameters: focal length $s = 2$, lens radius $R = 1$, and thickness of regular waveguide layer $d = 1.0665$. The other structure parameters were as follows: substrate (SiO_2) refractive index $n_s = 1.470$; refractive index of the first (regular) waveguide layer (Corning 7059 glass) $n_f = 1.565$,, refractive index of the second waveguide layer (Ta_2O_5

TGWLL) of variable thickness $h(y,z) - n_L = 2.100$; and refractive index of the coating layer (air) $n_c = 1.000$.

As can be seen in Fig. 3, the data obtained by us within the matrix model of the method of comparison waveguides practically coincide with Southwell's data. However, the numerical calculation showed that our solution has a much higher accuracy (at least, by three decimal places in comparison with Southwell's result). This is especially important for synthesising generalised Luneburg lenses, which require to take into account the edge effects (influencing, for example, the accuracy of Fourier transform of the lens).

5.3 Calculation of the vertical field distribution in TGWLL

An analysis of the field profiles obtained in the matrix model of comparison waveguides at closely located points of the TGWLL under consideration showed that the vertical distribution of the eigenmode electromagnetic field is gradually transformed during the motion of the mode phase front along a smoothly irregular TGWLL portion [4, 5]. The main difference of the vertical field distribution obtained in the zero-order vector approximation is that all amplitude coefficients $\{A_j\}$ and $\{B_j\}$ are simultaneously involved in the calculations; i.e., the modes are hybridised [1 – 5].

Figure 4 shows the field amplitudes $E_z(x)$ of the TM_1 mode (which demonstrate more clearly their change) at close points on the TGWLL dispersion curve (see also Fig. 1). It can be seen in these figures that the vertical distribution of the eigenmode electromagnetic field in the zero-order vector approximation of the adiabatic-mode method is gradually transformed during the motion of the eigenmode phase front from point to point along a smoothly irregular portion of a thin-film generalised waveguide Luneburg lens.

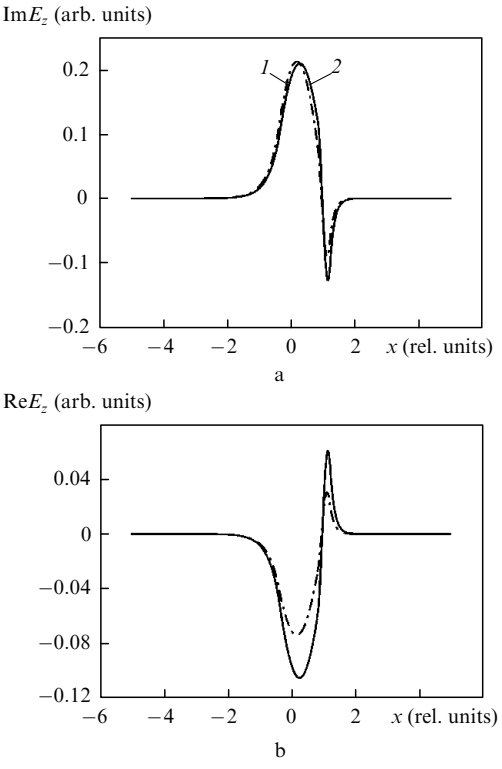

Figure 4. Amplitudes of the (a) imaginary and (b) real parts of the fields $E_z(x)$ at close points in the dispersion curve for the TM_1 mode of the TGWLL with (*1*) $\beta = 1.5384$, $d = 1.1850$ and $h = 0.3706$ and (*2*) $\beta = 1.5414$, $d = 1.1850$, $h = 0.3973$.

To calculate the vertical distribution of the eigenmode electromagnetic field in the first-order approximation, one must supplement the computational program with a procedure for calculating the first-order additives with respect to δ. The results of these calculations will be reported elsewhere.

Note that our estimation of the power loss for leaky modes propagating in the above-considered TGWLL showed good correspondence with the experimental data [14, 17]: the loss for a lens with a 1-cm radius is about 0.9 dB, which corresponds to a power loss of about 0.22 cm^{-1} on this lens. At this damping coefficient the power loss of waveguide modes on this full-aperture TGWLL will not exceed 20 %. A successive limitation of the lens aperture (at the edges, where the contribution of leaky modes is large) by 10 % and 20 % makes it possible to reduce the power loss by 15 % and 13 %, respectively. These estimates were obtained within the first-order approximation of the asymptotic method [3] and characterise the maximally possible power loss on such full-aperture TGWLLs.

6. Conclusions

We have numerically simulated for the first time propagation of eigenmodes through a TGWLL within the previously obtained analytical solution of the vector electrodynamic problem for a smoothly irregular four-layer 3D integrated optical waveguide.

The corresponding dispersion relation has been calculated, in particular, taking into account the shift of the propagation constants of hybrid modes. The vertical distribution of the electromagnetic field of a smoothely deformed mode in a TGWLL has been constructed. A full-aperture TGWLL has been synthesised in the zero-order vector approximation.

The methods considered here make it possible to perform (in the design stage) high-precision computer analysis of all features of operation of complex multilayer smoothly irregular integrated optical 3D elements of the TGWLL type that are most important for experimenters.

An undoubted advantage of the theoretical description, methods, and algorithms proposed here is that they can be generalised to smoothly irregular integral 3D structures composed of layers of dielectric or magnetic materials, materials with nonlinear properties, or metamaterials.

References

1. Sevast'yanov L.A., Egorov A.A. *Opt. Spektrosk.*, **105**, 632 (2008).
2. Egorov A.A., Sevastianov L.A., Sevastyanov A.L., Lovetskiy K.P. *ICO Topical Meeting on Optoinformatics/Information Photonics 2008* (St. Petersburg: ITMO, 2008) p. 231.
3. Egorov A.A., Sevast'yanov L.A. *Kvantovaya Elektron.*, **39**, 566 (2009) [*Quantum Electron.*, **39**, 566 (2009)].
4. Airyan E.A., Egorov A.A., Sevast'yanov A.L., Lovetskii K.P., Sevast'yanov L.A. Preprint No. R11-2009-120, JINR (Joint Institute for Nuclear Research).
5. Egorov A.A., Sevast'yanov A.L., Lovetskii K.P. *Vestn. RUDN, Ser. Mat., Inform., Fiz.*, (3), 55 (2009).

6. Egorov A.A., Sevast'yanov L.A., Sevast'yanov A.L., Stavtsev A.V. *Vestn. RUDN, Ser. Mat., Inform., Fiz.*, (1), 46 (2010).
7. Luneburg R.K. *Mathematical Theory of Optics* (Berkely: University of California Press, 1966).
8. Morgan S.P. *J. Appl. Phys.*, **29**, 1358 (1958).
9. Southwell W.H. *J. Opt. Soc. Am.*, **6**7, 1004 (1977).
10. Southwell W.H. *J. Opt. Soc. Am.*, **67**, 1010 (1977).
11. Katsenelenbaum B.Z. *Teoriya neregulyarnykh volnovodov s medlenno izmenyayushchimisya parametrami* (Theory of Irregular Waveguides with Slowly Varying Parameters) (Moscow: Izd-vo AN SSSR, 1961).
12. Shevchenko V.V. *Continuous Transitions in Open Waveguides: Introduction in Theory* (Golem: Boulder, CO, 1971; Moscow: Nauka, 1969).
13. Hunsperger R.G. *Integrated Optics: Theory and Technology* (Berlin: Springer, 1984; Moscow: Mir, 1985).
14. Vekshin M.M., Nikitin A.V., Nikitin V.A., Yakovenko N.A. *Avtometriya*, **45**, 102 (2009).
15. Khardikov V.V., Yarko E.O., Prosvirnin S.L. *Radiofiz. Radioastron.*, **13**, 146 (2008).
16. Snyder A.W., Love J.D. *Optical Waveguide Theory* (New York: Chapman and Hall, 1983; Moscow: Radio i Svyaz', 1987).
17. Anikin V.I., Deryugin L.N., Letov D.A., Polovinkin A.N., Sotin V.E. *Zh. Tekh. Fiz.*, **48**, 1005 (1978).
18. Shutyi A.M., Sementsov D.I., Kazakevich A.V., Sannikov D.G. *Zh. Tekh. Fiz.*, **69**, 74 (1999).